# STUDY OF THE WEAR BEHAVIOR OF AISI 304 AUSTENITIC STAINLESS STEEL USING RESPONSE SURFACE METHODOLOGY

**María Cristina Moré Farías**
Surface Phenomena Laboratory - Department of Mechanical Engineering - Polytechnic School of University of São Paulo
Av. Prof. Mello de Moraes, 2231 - São Paulo - SP - 05508-900, Brazil
e-mail: maria.farias@poli.usp.br

**Deniol Katsuki Tanaka**
Surface Phenomena Laboratory - Department of Mechanical Engineering - Polytechnic School of University of São Paulo
Av. Prof. Mello de Moraes, 2231 - São Paulo - SP - 05508-900, Brazil
e-mail: deniol.tanaka@poli.usp.br

**Amilton Sinatora**
Surface Phenomena Laboratory - Department of Mechanical Engineering - Polytechnic School of University of São Paulo
Av. Prof. Mello de Moraes, 2231 - São Paulo - SP - 05508-900, Brazil
e-mail: sinatora@usp.br

**Maria Elena Santos Taqueda**
Department of Chemical Engineering - Polytechnic School of University of São Paulo
Caixa Postal 61548, São Paulo - SP - 05424-970, Brazil
e-mail: santos.taqueda@poli.usp.br

***Abstract:*** *Rather than using the wear theories to determine a material wear rate as a function of contact conditions, the response surface methodology (RSM) was used as an alternative to the classical one-variable-at-a-time strategy to describe tribological behavior of materials. An attractive feature of using statistical design technique is that it requires few experimental procedures to set up dependence of the tribological parameters as a function of operating conditions.*

*In this investigation the non-lubricated wear mechanisms of AISI 304 austenitic stainless steel were studied at room temperature. Response surface methodology, using a second-order composite design for two factors was implemented. The independent variables were: applied load and sliding velocity. The wear rate of material was determined on a pin-on-disc machine, with applied load range from 6 N to 20 N and sliding speed range from 0.07 m/s to 0.81 m/s. Scanning electron microscopy (SEM) was used to characterize the worn surfaces and the debris particles morphologies.*

*The use of the experiment design, in addition to the reduction of the number of experiments, the statistical analysis and modeling provided useful and precise information to show the significance of the observed wear trends. A second-degree polynomial was used to represent a curved surface, which fits the experimental data, instead of two different straight lines for the wear rate. The analysis of the response surface for the wear rate and the characterization of worn specimens revealed a change of wear mechanism from oxidative wear to plastic deformation as a function of tangential speed and applied load.*

***Keywords:*** *sliding wear, austenitic stainless steel, response surface methodology*

## 1. Introduction

Austenitic stainless steels are used in nuclear reactor and more generally in the hot regions of chemical and power generation plants. These materials are considered to have poor wear characteristics, but its behavior depends on the wear conditions. Various works have been developed to study the dry sliding wear of these materials regarding the operational parameters, load, sliding speed and sliding distance, at different environment conditions.

Hsu *et al.* (1980) studied the wear behavior of AISI 304 and AISI 316 stainless steel blocks sliding against AISI 440C rings, at various levels of load (63, 133 and 200 N) and concluded that the greater tendency to form strain-induced $\alpha'$-martensite on the AISI304 steel was probably responsible for its poor wear behavior compared to the AISI 316 steel. Yang *et al.* (1985) results confirmed Hsu *et al.* (1980) observations where the sliding wear of 304 and 316 blocks against M2 tool steel was studied in the same range of applied load. Apart from the $\alpha'$-martensite induced by plastic deformation in the 304 steel, Yang *et al.* (1985) concluded that the nature of the transfer process and the relative hardness of the contacting bodies also affect the sliding wear behavior of the austenitic stainless steels.

Smith (1984) investigated the reciprocating wear of AISI 316 steel on itself as a function of the sliding distance in air at room temperature in the load range 8 to 50 N. A linear increase in the debris amount with the sliding distance was observed. Also, a change in the appearance of wear debris with load from powder debris particles to large thin flakes was observed. In an other work, Smith (1985) investigated the effect of the sliding

on the same material in the same contact geometry at low load (8 N). A transition from high to low values of wear rate was detected with the increase in sliding distance, which was associated with the appearance of a reddish brown phase in the wear debris, identified as a hydrated form of the hematite. The critical distance increased with sliding speed.

Additional investigations on the wear behavior of the AISI 316L austenitic stainless steel have been developed by Rainforth *et al.* (1992) to study the deformed microstructure generated during the sliding contact. The AISI 316L steel pins were tested in a load range 2 to 60 N against zirconia discs. The decrease in the wear coefficient ($mm^3/Nm$) with load was associated with oxidation wear mechanism. A further characterization showed that the oxide consisted of a non-equilibrium, oxygen-containing bcc nonocrystalline phase and an amorphous phase, retaining same F:Cr ratio of the initial structure (Rainforth *et al.*, 2002).

In the above cited works the wear behavior of austenitic stainless steels is generally studied as a function of one of the operating parameter, load, sliding speed or sliding distance. In the cases where two variables are studied, the interrelation between them is not clear. The use of the response surface methodology can be an alternative to the classical one-variable-at-a-time approach to describe the sliding wear behavior of materials, since it requires few experimental conditions. Also, this statistical technique reduces the difficulty of analysis and provides useful and precise information to show the acceptability of the wear results. This methodology has been used to characterize the tribological behavior of aluminum alloys (Mashal *et al.*, 2001) and carbon steels (Chou and Lin, 1999), but no work of austenitic stainless steels have been reported.

In the present work, an attempt was made to characterize the non-lubricated sliding wear behavior of the AISI 304 austenitic stainless steel at room temperature. A second-order central composite design for two factors was implemented. The material was tested on a pin-on-disc machine in the 6 to 20 N load range and 0.07 to 0.81 m/s tangential velocity range. The worn surfaces and debris particles were characterized by scanning electron microscopy and X-ray diffraction.

## 2. Experimental

### 2.1. Test conditions and procedure

The unlubricated sliding tests were performed in air at room temperature ($25 \pm 2\,^oC$) and controlled relative humidity ($55 \pm 3\,\%$) using 6 N to 20 N applied load range. The relative sliding speed between the contacting pin and disc surfaces was varied between 0.07 m/s and 0.81 m/s. A 22 mm wear track was used. The tests were stopped after 3,600 s. The wear experiments were carried out in a pin-on-disc model TE79 Plint & Partners wear machine. The machine is composed of a dead load system for the application of load and a load cell for the measurement of the friction force. The friction force signal was acquired at 10 Hz rate.

The wear specimens were 8 mm diameter and 21 mm long pins with a flat tip. As a counterbody, a 74 mm diameter discs with 8 mm thick was used. Before the test, each pin was ground finished by the successive use of abrasive papers with 320, 400 and 600 grit sizes, reaching a surface roughness (arithmetic average, Ra) of about $0.13 \pm 0.01\ \mu m$. The material for the pins and discs was AISI 304 austenitic stainless steel (18.50 % Cr and 9.5 % Ni). The hardness of the steel was $170\ \pm 5\ HV$ (measured with 30 kgf load). Before and after each test, the pin and disc were ultrasonically cleaned, dried and weighed to determine the mass loss by analytical balances with 0.0001 g (for pins) and 0.01 g (for discs).

The pins specimens and wear debris were examined by scanning electron microscopy (SEM) and the chemical composition was determined by energy-dispersive spectroscopy (EDX). The surface temperature was evaluated by means of thermocouple, inserted in the pin through 1 mm diameter hole at 2 mm from the contact surface.

### 2.2. Experiment design

For the present study, the independent variables were the applied load and the tangential velocity and the response variable was the wear rate. The response surface methodology was selected with the purpose of determining a relationship between the values of the wear rate of the AISI 304 austenitic stainless steel and the settings of the applied load and tangential velocity. A polynomial model (Eq. (1)) was used as relation between the wear rate and the applied load and tangential velocity.

$$Y = \beta_0 + \sum_{i=1}^{k} \beta_i X_i + \sum_{i=1}^{k} \beta_{ii} X_i^2 + \sum_{\substack{i=1 \\ j>i}}^{k-1} \sum_{j=2}^{k} \beta_{ij} X_i X_j + \varepsilon \tag{1}$$

where:

$X_1, X_2, ..., X_k$ are the input variables which affect the response $Y$;
$\beta_0, \beta_i (i = 1, 2, ..., k), \beta_{ij} (i = 1, 2, ..., k; j = 1, 2, ..., k)$ are the unknown parameters, and
$\varepsilon$ is a random error.

A central composite design (CCD) proposed by Box and Hunter (1957) was used in order to describe the response surface of the wear rate and estimate the parameters in the second-order model (Eq. (1)). The kernel of such design is a complete $2k$ factorial design, where each of independent variables has two levels or values, which are coded as $-1$ and $+1$ values. This is denominated the factorial portion of the design. $2k$ star points positioned on the coordinate axes of factorial part $(\pm\alpha, 0, ..., 0)$ $(0, 0, \pm\alpha, 0, ..., 0)$ ... $(0, 0, ..., 0, \pm\alpha)$ were added to this design, where $\alpha$, is the distance from the center point of the design to a star point. This portion is called the axial portion of the design. Also, $n_0$ runs are added at the center point of the design.

In the present investigation, there are two independent input variables ($k = 2$) and, in this case, the experiment design contains N=14 unique points, where $n_0 = 6$ and $\alpha = \sqrt{2}$ were chosen as indicated by Khuri and Cornell (1987). A graphical representation of such two-factors composite design is illustrated in Fig. (1).

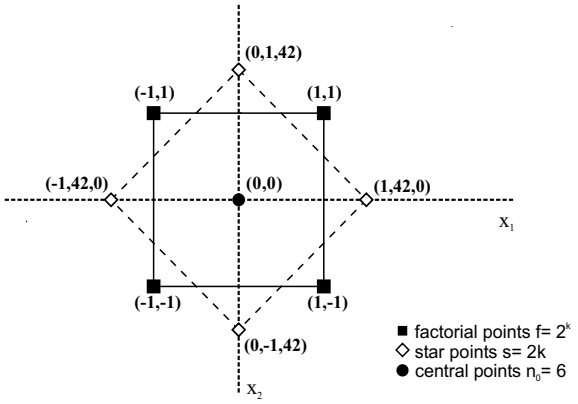


Figure 1. Central composite design with two factors ($k = 2$).

The first step of the strategy to develop the empirical model was to postulate a first-order polynomial relationship. For this purpose a first-order factorial design was used, which was composed by the factorial portion of the CCD plus three central points. A second-order model was more appropriate to describe the relationship of interest because a curvature was detected in the wear rate response surface. Thus, the next step was to perform additional experiments, one at each of the four axial combinations (i.e. the axial portion was added to the factorial portion of the design). These four additional test settings along with the four factorial test combinations, plus six central replicated points compose the central composite design. Finally, the experimental values of the wear rate from the CCD were fitted to the second-order polynomial Eq. (1). The stages of the response surface methodology were described by Box *et al.* (1978) and Khuri and Cornell (1987).

The original and coded values of the input variables are listed in Tab. 1. Although the six central points repetitions can be used to obtain an estimate of error, each of the eight runs of the factorial and axial part was repeated three times for better estimation of the experimental error and reliable evaluation of the parameters of the second-order model (Khuri and Cornell, 1987). However, given that the total number of experiments was large, the wear test could not be performed in the same day in homogeneous conditions. Under such circumstances, a way to improve the precision was grouping or blocking the repetitions (Robert and Virgil, 1984; Peter, 1971). As a result, more homogeneous conditions within the block were obtained and the experimental error was reduced.

Table 1. Original and coded values of independent variables.

| | coded values | | | | |
|---|---|---|---|---|---|
| | $-\sqrt{2}$ | -1 | 0 | 1 | $\sqrt{2}$ |
| | original values | | | | |
| applied load F (N) | 6 | 8 | 13 | 18 | 20 |
| tangential velocity V (m/s) | 0.07 | 0.18 | 0.44 | 0.70 | 0.81 |

## 3. Results and discussions

### 3.1. Wear rate regression

Table (2) shows the original and coded values of input variables. The pin specimens wear rate response values at each applied load and tangential speed values combinations are also shown. The wear rate (Q, mass per unit of time, g/s) was calculated from the mass loss of each pin specimen divided by the time. The wear rates values listed in Tab. (2) represent the average of three test repetitions. The second-order polynomial fitted

from experimental wear rate values along with the combinations of the coded variables is represented by the following equation:

$$\widehat{Q}(f,v) = 18.96 + 1.97f - 2.26f^2 + 3.79v - 5.64v^2 - 0.56fv \tag{2}$$

where multiplication factor is $10^{-6}$ (g/s) and $f$ and $v$ are coded values of the applied load and tangential velocity, respectively. The second-order polynomial can be expressed in original variables by de-coding Equation (2), using the following equation:

$$x_{ui} = \frac{X_{ui} - \overline{X_i}}{S_i}\ , i = 1, 2, ..., k \tag{3}$$

where $X_{ui}$ is the actual level in the original units of the $i^{th}$ factor for the $u^{th}$ experimental run, $\overline{X_i}$ is the average of the low and high levels for the $i^{th}$ factor, and $S_i$ is the range between the low and high levels divided by two. Thus, the wear rate equation (with multiplication factor $10^{-6}$ (g/s)) as a function of the original values of applied load ($F$) and tangential velocity ($V$) is given by:

$$\widehat{Q}(F,V) = -26.65 + 3.00F - 0.09F^2 + 92.62V - 82.42V^2 - 0.43FV \tag{4}$$

Table 2. The experimental design points and the resulting experimental and predicted values of the wear rate for the central composite design.

| | original values | | coded values | | |
|---|---|---|---|---|---|
| run | applied load $F$ (N) | tangential velocity $V$ (m/s) | applied load $f$ | tangential velocity $v$ | experimental wear rate $Q$ (g/s) $\times 10^{-6}$ |
| 1 | 8 | 0.18 | -1 | -1 | 5.08 |
| 2 | 18 | 0.18 | 1 | -1 | 8.31 |
| 3 | 8 | 0.70 | -1 | 1 | 13.90 |
| 4 | 18 | 0.70 | 1 | 1 | 14.91 |
| 5 | 20 | 0.44 | $\sqrt{2}$ | 0 | 19.03 |
| 6 | 6 | 0.44 | $-\sqrt{2}$ | 0 | 10.89 |
| 7 | 13 | 0.81 | 0 | $\sqrt{2}$ | 13.47 |
| 8 | 13 | 0.07 | 0 | $-\sqrt{2}$ | 2.94 |
| 9 | 13 | 0.44 | 0 | 0 | 18.44 |
| 10 | 13 | 0.44 | 0 | 0 | 17.97 |
| 11 | 13 | 0.44 | 0 | 0 | 19.47 |
| 12 | 13 | 0.44 | 0 | 0 | 17.61 |
| 13 | 13 | 0.44 | 0 | 0 | 20.33 |
| 14 | 13 | 0.44 | 0 | 0 | 18.83 |

The polynomial was tested by the analysis of variance (ANOVA) using a statistical program. As shown in Tab. (3), the lack of fit is not significant. The value of lack of fit test statistic is:

$$F = \frac{\text{Lack of fit mean square}}{\text{Pure error mean square}} = \frac{2.42}{1.01} = 2.40$$

Since the value $F = 2.40$ does not exceed the table value $F_{(0.05,17,5)} = 4.62$, there is no evidence of the lack of fit of the tested model.

The degree of significance of the second-order model in Eq. (2) was determined by testing the null hypothesis, $H_0 : \beta_{11} = \beta_{22} = 0$, or by testing if both the applied load and the tangential speed have no effect on the wear rate of the AISI 304 pin.

The calculated value:

$$F = \frac{\text{Regression mean square}}{\text{Residual mean square}} = \frac{172.86}{2.10} = 82.49$$

is five times higher than the table value $F_{(0.05,5,22)} = 2.66$, as stated by Box and Draper (1987). In other words, one or both parameters, $\beta_{11}$ and $\beta_{22}$, in Eq. (1) are not equal to zero.

Thus, the model is significant, which means that surface curvature is present in the observed values of the wear rate of the AISI 304 austenitic stainless steel.

With the purpose of checking the individual effects of the factors used in the experiment a hypothesis test was performed by comparing each parameter in the fitted model to its respective estimated standard error. In this case, a test of the null hypothesis, $H_0 : \beta_i = 0$, was performed by calculating the values of the test statistic

$$t = \frac{b_i}{\sqrt{\widehat{Var}(b_i)}} \tag{5}$$

and comparing this value (absolute value) with the t-table value, $t_{\alpha,\nu}$. In the Eq. (5) $b_i$ is the estimated regression coefficient (taken from Eq. (2)) and $\sqrt{\widehat{Var}(b_i)}$ is the estimated standard error of $b_i$ (taken from Tab. (3)). As shown in Tab. (3), the two-interaction regression coefficient ($fv$) is non-significant and the final form of the fitted equation for the wear rate is:

$$\widehat{Q}(f,v) = 18.96 + 1.97f - 2.26f^2 + 3.79v - 5.64v^2 \tag{6}$$

$$\widehat{Q}(F,V) = -24.20 + 2.81F - 0.09F^2 + 87.06V - 82.42V^2 \tag{7}$$

Table 3. Analysis of variance for the wear rate second-order fitted model.

| Source of variation | Some of squares SS ($\times 10^{12}$) | Degrees of freedom df | Mean square MS ($\times 10^{12}$) | F-ratio F | $F_{(\alpha,\nu_1,\nu_2)}$ F-table | Probability p |
|---|---|---|---|---|---|---|
| Blocks | 0.51 | 2 | 0.26 | 0.26 | | 0.784409 |
| f (linear) | 93.09 | 1 | 93.09 | 92.60 | | 0.000205 |
| f (quadratic) | 54.44 | 1 | 54.44 | 54.16 | | 0.000727 |
| v (linear) | 344.59 | 1 | 344.59 | 342.80 | | 0.000008 |
| v (quadratic) | 338.89 | 1 | 388.89 | 337.12 | | 0.000009 |
| fv (cross-product) | 3.71 | 1 | 3.71 | 3.70 | | 0.112427 |
| Total regression | 864.30 | 5 | 172.86 | 82.49 | 2.66[a] | |
| Lack of fit | 41.07 | 17 | 2.42 | 2.40 | 4.62[b] | 0.168912 |
| Pure error | 5.03 | 5 | 1.01 | | | |
| Total error | 46.10 | 22 | 2.10 | | | |
| Total | 910.40 | 29 | | | | |

$\%R^2 = SQ_R/SQT * 100 = 94.94\ \%$

| Parameter | df | Estimate ($\times 10^{-6}$) | Std err. ($\times 10^{-6}$) | t-ratio[c] | p |
|---|---|---|---|---|---|
| Mean/Intercept | 1 | 18.96 | 0.72 | 26.20 | 0.000000 |
| f | 1 | 1.96 | 0.30 | 6.67 | 0.000001 |
| $f^2$ | 1 | -2.26 | 0.44 | -5.10 | 0.000042 |
| v | 1 | 3.79 | 0.30 | 12.82 | 0.000000 |
| $v^2$ | 1 | -5.64 | 0.44 | -12.72 | 0.000000 |
| fv | 1 | -0.56 | 0.42 | -1.33 | 0.196420 |

[a] is the value of the F-ratio for the significance level $\alpha = 0.05$ and degrees of freedom 5 and 22 ($F_{(0.05,5,22)}$).
[b] is the value of the F-ratio for the significance level $\alpha = 0.05$ and degrees of freedom 17 and 5 ($F_{(0.05,17,5)}$).
[c] is the value of the Student's t-distribution for $\alpha = 0.05$ and 22 degrees of freedom associated with the residual mean square ($t_{0.025,22} = 2.074$).

The estimated regression coefficients can be considered as a measure of the effects of the variables on the wear rate. It means that stronger the effect higher will be the regression coefficient. From Eq. (6) it is possible to note that the tangential velocity (factor $v$) has the strongest effect on the wear rate and, since the quadratic estimated coefficient of both the applied load and the tangential velocity are negative, the wear rate response surface reaches a peak and then decreases.

This behavior is shown in Fig. (2) by means of a three-dimensional curve and a contour plot of the estimated wear rate surface. The increase, in both the applied load and the tangential speed, produces higher values of wear rate up to maximum point (about (16 N, 0.54 m/s)) from which the wear rate decreases.

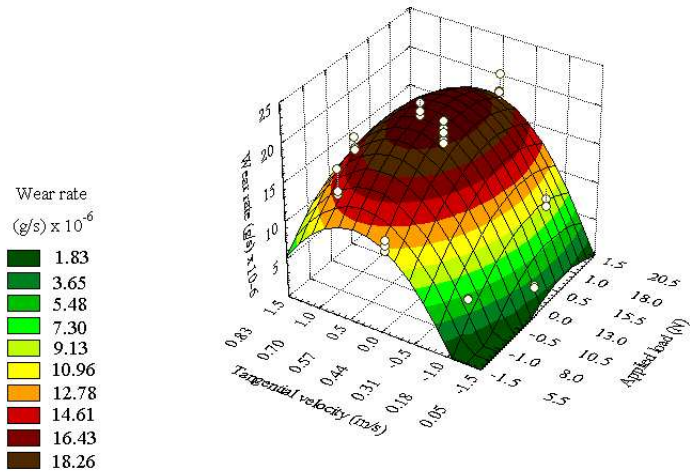


(a)

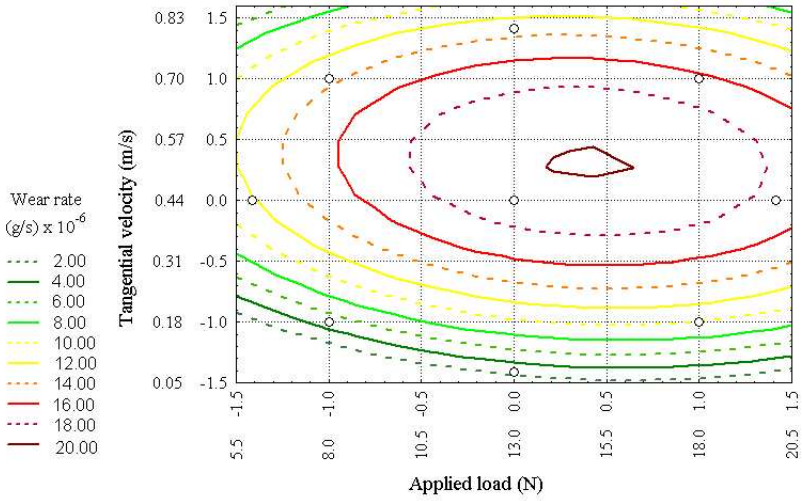


(b)

Figure 2. (a) Response surface and (b) contour plot of the estimated wear rate response surface. The (∘) symbols indicate the test conditions used in the model of RSM.

### 3.2. Wear debris and wear surfaces

The change in the appearance of the debris particles noticeable, and it was confirmed by the scanning electron microscopy analysis. The wear debris formed at moderate test conditions (runs 1 to 2 and 8, see Tab. (2)) were fine dark powder, while for severe conditions (runs 3 to7 and 9-14) consisted of larger particles with metallic appearance.

Figure (3(a)) shows the appearance of the debris obtained at 8 N and 0.18 m/s. It can be observed that the wear particles size was less than 2 $\mu m$ approximately. They also comprised some fragments of metallic particles sizes larger than 4 $\mu m$, which was probably formed in the initial stage of sliding. The size of the metallic debris obtained at severe test conditions was much greater than that of the dark powder debris ($\approx 200\ \mu m$). Figure (3(b)) shows the typical wear particles obtained at 18 N and 0.70 m/s test. Different types of morphologies were observed in the metallic debris produced at severe wear conditions, i.e. irregular plates with lamellar structure and particles with cylindrical and spherical shape. From Fig. (4(a)) it seems that the particles retained within the interface experienced work-hardening, that is, these particles deformed and rolled to form a cylindrical or spherical debris. Additionally, it is possible to observe in Fig. (4(b)) that the irregular plates might fracture into finer fragments, which further deformed, rolled-up or broke up subsequently.

The appearance of the worn scar analyzed by SEM is illustrated in Fig. (5). At moderate conditions (test 1, 2 and 8) the worn surfaces were composed of regions with a dark film of similar appearance to the fine dark wear debris. In addition, even in the region where the oxidation seemed to occur, plastic deformation of the surface was also observed. It is possible that an oxidized layer was formed on previously deformed

regions. Non-conducting particles adhered in the surface were also observed. At severe test conditions a change in the characteristic of the wear scar was noticed. The surface showed metallic appearance and considerable plastic deformation. The deformed material seemed to be displaced in the sliding direction forming regions with a multilayered structure. The worn surfaces were also composed by grooves, probably caused by entrapped metallic plate particles, as is shown in Fig. (6).

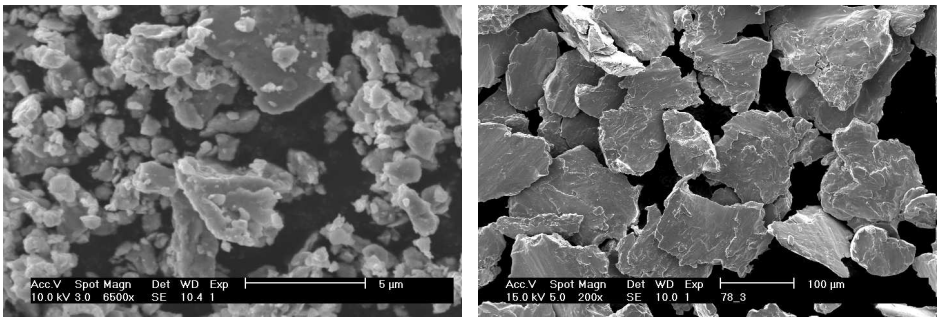


(a) (b)

Figure 3. Secondary electron images of the wear debris obtained at: (a) 8 N and 0.18 m/s and (b) 18 N and 0.70 m/s.

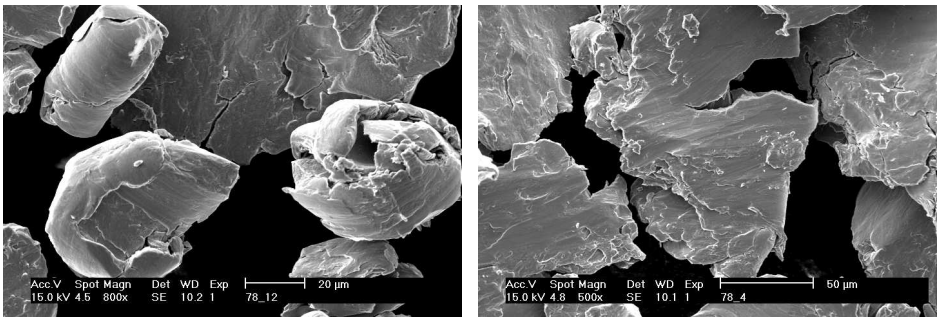


(a) (b)

Figure 4. SEM images of the wear debris obtained at 18 N and 0.81 m/s (a) cylindrical wear debris; (b) the breaking up of a plate wear particle.

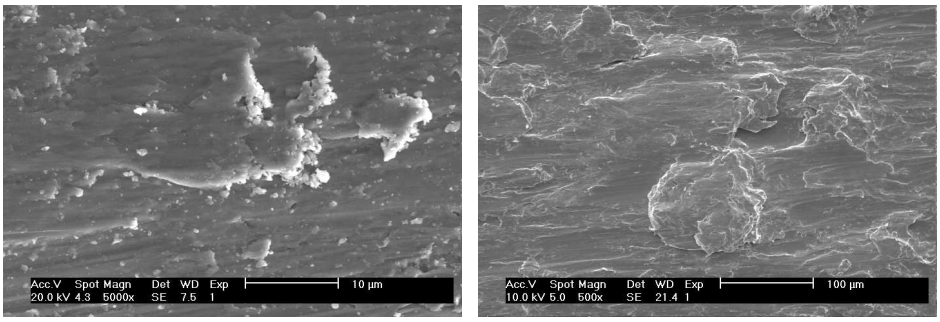


(a) (b)

Figure 5. Worn surface of the AISI 304 steel tested at (a) 8 N, 0.18 m/s; (b) 13 N, 0.44 m/s.

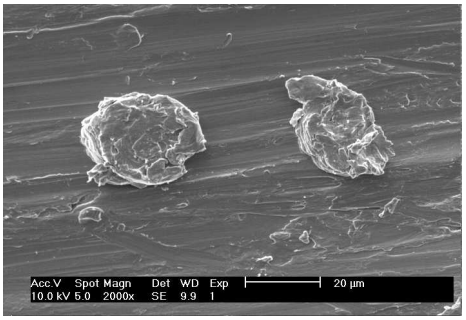


Figure 6. Wear scar on pin at 13 N and 0.44 m/s showing a groove formed by an entrapped metallic particle.

EDX analysis of dark particles, obtained at moderate test conditions, indicated that the oxygen amount was significant. On the other hand, the ratio of Fe: Cr: Ni was the same, and the X-ray diffraction did not detect the oxide presence. Therefore, from these results, it is not possible to conclude that these particles were oxidized. Some researchers have reported the presence of oxide in the wear debris and the occurrence of mild wear due to the oxide film formation in the wear scars of austenitic stainless steel specimens (Smith, 1985; Rainforth *et al.*, 2002; Straffelini *et al.*, 2002). According to Jiang *et al.* (1994), for iron or steels, an oxide film with thickness of 2 $nm$ can form within 0.1 s at 20 $^o$ C in air. Such tin oxide film is not possible to be detected by conventional X-ray diffraction technique.

Stott *et al.* (1995) presented a model that takes into account the oxide generation during the low-speed (less than 1 m/s) sliding wear and its influence in the wear rate of alloys, assuming that oxide could be generated by oxidation of metal asperities (in the same manner as the mild-oxidational wear model defined by Lim and Ashby (1987) or by oxidation of metallic debris. The extent of oxidation depends on the temperature at asperity contacts, time of contact and oxidation characteristics of the metal.

For the present work, the low surface temperature (25 $^o$C), obtained under moderate test conditions, indicate that the oxidation is more probable to occur by particle oxidation than by growing of oxide film on the surface. This process may occur at temperatures slightly above 20 $^o$ C.

The explanation to the severe wear results for runs 3 to 7 and 9 to 14, (Tab. (2)) is the occurrence of considerable plastic deformation and large amount of material removal from the contact surface, producing metallic appearances of the wear tracks and detached fragments.

The analysis of the sliding wear of AISI 304 with applied load and tangential velocity at severe wear conditions is more complex. It is known that the plastic deformation, strain-induced martensite formation, material transference, are responsible for the formation a hard surface (Yang *et al.*, 1985; Rigney, 1992; Rigney, 2003).

The maximum in the wear rate observed in Fig. (2) can be explained by the increase in surface temperature and strain of subsurface with applied load and tangential speed. In this case, the effect of the tangential velocity is more significant, according to Eq. (6) and Fig. (2(a)). Due to the considerable ductility of the AISI 304 steel, the increase in tangential velocity, above a critical value, can induce a thermal softening of the surface, which reduces the strain hardening and the tendency to form $\alpha$'-martensite, promoting the formation of a less brittle surface layer (Hsu *et al.*, 1980). As a consequence, the removal of metallic fragment from the interface becomes more difficult and the wear rate is reduced.

## 4. Summary and conclusions

a) The dry sliding wear behavior of AISI 304 austenitic stainless steel was studied at room temperature with 6 N to 20 N applied load and 0.07 m/s to 0.81 m/s tangential velocity, by means of response surface methodology statistic technique to verify the significance and influence of testing parameters on the wear of austenitic stainless steels.

b) The observed wear rate depends on applied load and tangential speed intensities and the second-order model showed that the tangential speed had a major influence on the wear of the AISI 304 steel.

c) The experimental data were successfully represented by a second-order polynomial model, determined by using the central composite experimental design.

d) The adjusted regression equation was able to determine the sliding condition for the transition to severe wear regime. The critical point could be related to the change in the mechanical properties of the tested material rather than to a transition of wear mechanism.

e) The AISI 304 stainless steel showed a change in the wear mechanism from a metallic debris oxidation to a plasticity-dominated mechanism.

## 5. Acknowledgement

The authors acknowledge FAPESP (São Paulo State Research Support Foundation) for research support (98/15987-3).

## 6. References

Box, George E. P. and Norman R. Draper, 1987, "Empirical model-building and response surfaces", Wiley series in probability and mathematical statistics, Applied probability and statistics, Wiley. New York.

Box, George E.P., William G. Hunter and Stuart J., 1978, "Statistics for experimenters. An introduction to design, data analysis and model building", John Wiley. New York.

Box, G.E.P. and J.S. Hunter, 1957, "Multi-factor experimental designs for exploring response surfaces", Annals of Mathematical Statistics, Vol. 28, No. 1, pp. 195–241.

Chou, C. C. and L. F. Lin, 1999, "Application of the response surface method to the tribological analysis of a medium-carbon steel under mild-oxidation wear", Journal of Tribology, Transactions of the ASME, Vol. 121, pp. 185–197.

Hsu, K. L., T. M. Ahn and D. A. Rigney, 1980, "Friction wear and microstruture of unlubricated austenitic stainless steels", Wear, Vol. 60, No. 1, pp. 13–37.

Jiang, J. R., F. H. Stott and M. M Stack, 1994, "Some frictional features associated with the sliding wear of the nickel-base alloy N80A at temperatures to 250 $^o$C", Wear, Vol. 176, No. 2, pp. 185–194.

Khuri, André I. and John A. Cornell, 1987, "Response surfaces. Designs and analyses", Vol. 81 of Statistics, textbooks and monographs, Marcel Dekker, Inc. ASQC, New York.

Lim, S. C. and M. F. Ashby, 1987, "Wear-mechanism maps", Acta metallurgical, Vol. 35, No. 1, pp. 1–24.

Mashal, Y. A-H., M. H. El-Axir and M. A. Kassem, 2001, "The machinability and tribological characteristics of aluminum alloys with improved elevated temperature properties using rapidly solidified powder", Wear, Vol. 250, pp. 518–528.

Peter, W. M. John, 1971, "Statistical design and analysis of experiments", New York: Macmillan.

Rainforth, W. M., R. Stevens and J. Nutting, 1992, "Deformation structures induced by sliding contact", Philosophical Magazine A, Vol. 66, pp. 621–641.

Rainforth, W.M., A.J. Leonard, C. Perrin, A. Bedoll-Jacuinde, Y. Wang, H. Jones and Q. Luo, 2002, "High resolution observations of friction-induced oxide and its interaction with the worn surface", Tribology International, Vol. 35, No, 11, pp. 731–748.

Rigney, D. A., 1992. "Some thoughts on sliding wear", Wear, Vol. 152, No. , pp. 187–192.

Rigney, D. A., 2003, "Transfer, mixing ans associated chemical and mechanical processes during the sliding of ductile materials", Wear, Vol. 245, No. 1-2, pp. 1–9.

Robert, A. McLean and L. Anderson Virgil, 1984, "Applied factorial and fractional designs", New York: M. Dekker.

Smith, A. F., 1984, "The friction and sliding wear of unlubricated 316 stainless steel at room temperature in air",Wear, Vol. 96, No. 3, pp. 301–318.

Smith, A. F., 1985, "The influence of surface oxidation and sliding speed on the unlubricated wear of 316 stainless steel at low load", Wear, Vol. 105, No. 2, pp. 91–107.

Stott, F. H., J. Jiang and M. M. Stack, 1995, "A mathematical model for sliding wear of metals at elevated temperatures", Wear, Vol. 181-183, No. 1, pp. 20–31.

Straffelini, G. D., Trabucco and A. Molinari, 2002, "Sliding wear of austenitic and austenitic-ferritic stainless steels", Metallurgical and materials transactions A-physical metallurgy and materials science, Vol. 33 No, 3, pp. 613–624.

Yang, Z.Y., M. G. S. Naylor and D. A. Rigney, 1985, "Sliding wear of 304 and 310 stainless steels", Wear, Vol. 105, No. 6, pp. 73–86.

## 7. Copyright notice